

Graph theoretical analysis based on EEG effective connectivity in ADHD children

Mingkan Shen (✉ Mingkan.Shen@usq.edu.au)

University of Southern Queensland <https://orcid.org/0000-0002-6770-4366>

Paul Wen

University of Southern Queensland

Yan Li

University of Southern Queensland

Bo Song

University of Southern Queensland

Research

Keywords: ADHD, EEG, effective connectivity, MVAR, PSI, graph theory

Posted Date: April 1st, 2021

DOI: <https://doi.org/10.21203/rs.3.rs-375557/v1>

License: © ⓘ This work is licensed under a Creative Commons Attribution 4.0 International License.

[Read Full License](#)

Abstract

This paper reports a new method to identify the ADHD children using EEG signals and effective connectivity techniques. In this study, the original EEG data is pre-filtered and divided into Delta, Theta, Alpha and Beta bands. And then, the effective connectivity graphs are constructed by applying independent component analysis, multivariate regression model and phase slope index. The measures of clustering coefficient, nodal efficiency and degree centrality in graph theory are used to extract features from these graphs. Statistical analysis based on the standard error of the mean are employed to evaluate the graph theory measures in each frequency band. The results show a decreased average clustering coefficient in delta band for ADHD subjects. Also, in delta band, the ADHD subjects have increased nodal efficiency and degree centrality in left forehead part and decreased in forehead middle.

1 Introduction

Attention deficit hyperactivity disorder (ADHD) is a heterogeneous disease with a high prevalence. The prevalence of children worldwide is estimated to be 8%-12%, and about 60% of symptoms and their effect continue into adulthood [1, 2]. In recent years, researchers have used brain Computed Tomography (CT), magnetic resonance imaging (MRI), functional magnetic resonance imaging (fMRI), magnetoencephalography (MEG), electroencephalography (EEG) and other methods to conduct in-depth research on the microstructure of the brain [3–6]. The development of the detection method encouraged the researchers to gain deeper information in ADHD [7]. The brain structure, cerebral blood flow, brain electrical activity, gene structure, executive ability and cognitive ability of children with ADHD are significantly different from those of normal children, and this difference exists for a long time [8]. EEG is a popular and widely used measurement technique for extracting information from brain. It also is a non-invasive nerve discharge detection technology with millisecond-level high time resolution [9]. Visual inspection of the EEG signal is a method to detect the ADHD [10–12].

One of the methods for detecting ADHD is functional connectivity. The Functional connectivity represents the statistical correlation of the functional activities of different brain regions in time courses, and the statistical calculation is performed based on EEG signal [13–15]. Effective connectivity also called the directed functional connectivity which provided the causal information between each brain regions [16–18]. At present, most methods of calculating effective connectivity are based on parameter models, such as Granger causality model, dynamic causality model and multivariate regression (MVAR) model [19–21]. Graph theory is the main mathematical tools used in the brain connectivity analysis, the measures of the graph theory describe the local and global features of the brain network [22]. Most of the brain connectivity in ADHD children were focused on the degrees, clustering coefficient, shortest path length, centrality and efficiency [2, 23].

MVAR model is used to fit the Granger causality model because it can infer the causal information between each brain region [24]. However, the Granger causality algorithm has the limitation in constructing effective connectivity which exists volume conduction problem [25]. To overcome this

limitation, we proposed the phase slope index (PSI) measure to construct effectivity in our study. Most PSI measure is based on the power spectrum analysis because this algorithm refers to the change of phase differences as a function of frequency [26]. To get more high frequency resolution in frequency domain output, we used the MVAR model to represent the power spectrum analysis.

In this study, we used the PSI algorithm based on the MVAR model to construct the effective connectivity. We applied the connectivity matrix as the graph to extract the features by three graph theory measures clustering coefficient, nodal efficiency and degree centrality. At last we used the standard error of the mean (SEM) to get the statistical results between ADHD and health control (HC).

2 Method

The framework of the proposed method is shown in Fig. 1, which indicates how to use effectivity connectivity to detect the ADHD and HC progress. At first, the 19 channels EEG raw data is collected from ADHD and HC subjects during a visual attention task. Then, the pre-processing is conducted to remove the artifacts and noise from the raw data. The MVAR model and PSI algorithm are applied to construct a connectivity matrix ($19 \times 19 \times 4$) in delta (0.5–4 Hz), theta (4–8 Hz), alpha (8–13 Hz) and beta (13–30 Hz) frequency bands for each subject. Furthermore, graph theoretical analysis is proposed to extract the features from the connectivity matrix (graph) as global efficiency and clustering coefficient. At last, we conducted the statistical analysis by applying the SEM algorithm.

2.1 Dataset

To validate the performance of the classification between ADHD and HC in this study, the EEG data for ADHD and HC from IEEE Data port (DOI: 10.21227/rzfh-zn36) has been used. According to DSM-IV criteria, participants were 30 children with ADHD (15 boys and 15 girls, ages 7–12) provided by Roozbeh hospital in Tehran, Iran and 30 HC subjects were (15 boys and 15 girls, ages 7–12) collected from a primary school. All children of HC group have not got a history of psychiatric brain disorder such as epilepsy, major medical illness or any report of high-risk behaviors.

The EEG raw data was collected from a 10–20 standard 19 channels electrode cap which correspond to FP1, FP2, F3, F4, C3, C4, P3, P4, O1, O2, F7, F8, T7, T8, P7, P8, Fz, Cz, Pz respectively. The data has a 128 Hz sample rate and with two reference electrodes A1 and A2.

2.2 EEG pre-processing

EEG signals were filtered in bandpass frequency bands between 0.5 Hz to 50 Hz using a zero-phase finite impulse response (FIR) filtering algorithm. Independent component analysis (ICA) is used to assume statistically independent sources, in addition, removing the blinks, eye-movements and artifacts in this step. Then, we re-referenced the data to the average of all scalp channels.

2.3 Multivariate autoregressive (MVAR) models

MVAR model can infer directivity and the causal relationship between brain connections based on effective connectivity methods which is an extension of AR model on multi-dimensional variables [21]. The algorithm of MVAR model is shown as follow:

$$X(n) = \sum_{k=1}^p A(k) \times X(n-k) + W(n)$$

1

$X(n) = [x_1(n), \dots, x_M(n)]^T$ is the current value of EEG pro-processing signal in time n . M is the channel number, here M equals to 19. p is the model order, $A(k)$, $k = 1, \dots, p$, are $M \times M$ coefficient matrix of MVAR model which describe the linear interaction at lag k from $x_j(n-k)$ to $x_i(n)$, ($i, j = 1, \dots, M$).

$W(n)$ is a vector of zero-mean Gaussian noise process with covariance matrix Σ . Here we use the multichannel Yule-Walker equation to describe the relationship between the coefficient matrix $A(k)$ and covariance matrix Σ because its simple calculation and good performance [27]. Thus, the output of the $X(n)$ is the $19 \times 19 \times p$ matrix of each subject.

Another key parameter of the MVAR model is the order of the MVAR model. The choice of order is closely related to the fitting effect of the model. The small order cannot make full use of the information of the observation data for accurate fitting. The large order would cause the phenomenon of overfitting and would increase the expense of calculation.

In this study, Akaike Information Criterion (AIC) equation is provided to assess the order of MVAR model [28].

$$AIC(p) = \ln|\Sigma(p)| + \frac{2}{N}mp^2$$

2

where $\Sigma(p)$ represents the covariance matrix of fitting error of the p -order model, and N represents the total number of settlements used for model fitting. Thus, $p = 5$ was selected as the model order according to the AIC equation.

We also need to obtain frequency domain data through coherent spectrum estimation, where the MVAR model is converted to frequency domain form through Fourier transform. The transfer matrix of MVAR model $H(f)$, and cross-spectrum matrix $S(f)$ are estimated as follow:

$$H(f) = \left(\sum_{k=0}^p -A_k e^{-jk2\pi f} \right)^{-1}$$

3

$$S(f) = H(f) \Sigma \left(H^H(f) \right)$$

4

where $H^H(f)$ is the conjugate transpose of $H(f)$. Σ is the noise covariance matrix. A_k is the parameter of $M \times M$ coefficient matrix and the p is the number of model order.

We use the MVAR model to obtain more refined spectral analysis results, which is conducive to more accurate calculation of effective connectivity coefficients. The spectrum power values were calculated in whole frequency band. After the MVAR model fitting, we got a $19 \times 19 \times 128$ matrix for each subject, this is also the input of the PSI algorithm in Eq. (6).

2.4 Effective connectivity analysis

Phase slope index measure is used in our study. The PSI between two given components signals 'i' and 'j' is defined as:

$$PSI_{ij} = I(\sum_{f \in F} C_{ij}^*(f) C_{ij}(f + \delta_f))$$

5

where F is the set of frequencies of interest, F equals to half-bandwidth of the integration across frequencies. C is the normalized coherent spectrum and δ_f is an incremental step in the frequency domain. The normalized coherent spectrum C is defined as:

$$C_{ij}(f) = \frac{|S_{ij}(f)|}{\sqrt{S_{ii}(f) S_{jj}(f)}}$$

6

The definition of $S_{ij}(f)$ means the cross-spectrum between i and j , and it is the output of the Eq. (4).

According to the definition in Eq. (6), the imaginary part of coherent spectrum is used in this algorithm. Because the imaginary part information of the coherent spectrum would not change due to aliasing between the signals [29]. In other words, PSI can avoid erroneous estimation in effective connectivity caused by signal aliasing.

In this study, we used to construct the effective connectivity in four frequency band which delta (0.5–4 Hz), theta (4–8 Hz), alpha (8–13 Hz) and beta (13–30 Hz) respectively between ADHD and HC. An average effective matrix for an ADHD subject and a HC subject of delta band was shown in Fig. 2 and Fig. 3.

2.5 Graph theoretical analysis

Two key parameters of the graph are the nodes and edges. To detect the ADHD, we use three graph theory measures: clustering coefficient, nodal efficiency and degree centrality.

Threshold method

Regarding to not all connection is necessary to be calculated in the graph theory, threshold method is used in weighted graph analysis. But threshold method has issue with threshold selection. A higher threshold may cause the problem of not being able to construct a brain network and a lower threshold may cause the problem of no meaningful connectivity measures [30]. Empirically, selecting threshold as 0.2 produced the best results.

Clustering coefficient

Clustering coefficient is proposed to assess the ability of segregation in graph which is the most important measures in researching cognitive problem of brain [31]. The algorithm is shown as follow [22]:

$$C^W = \frac{1}{N} \sum_i \frac{2t_i^w}{k_i(k_i - 1)}$$

7

The t_i^w is the number of triangles around a node i , a subgraph with three nodes and three edges is called a triangle. k_i is the degree of a node i . N is the numbers of nodes, here N equals to 19. The algorithm of the t_i and k_i s described in Eqs. (8) and (9).

$$t_i^w = \frac{1}{2} \sum_{j, h \in N} (w_{ij}w_{ih}w_{jh})^{\frac{1}{3}}$$

8

$$k_i = \sum_{j \in N} w_{ij}$$

9

where w_{ij} is the connection weights between node i and node j . When the measures of edges from the graph are greater than the threshold value, the connection is defined existed and w_{ij} equals to the value of the edges, otherwise $w_{ij} = 0$.

Nodal efficiency

Nodal efficiency of a graph measures the ability of each node to exchange information, and is defined as [22]:

$$E_{nodal}(i) = \frac{1}{N-1} \sum_{i \neq j} \frac{1}{l_{ij}}$$

10

where N is the number of the nodes in the graph, and l_{ij} is a path between nodes i and j with the minimum number of edges.

Degree Centrality

Degree centrality of a graph measures the direct impact of the brain region on other adjacent brain regions [22]. The degree centrality formula shown as follow:

$$C_d(i) = \sum_{j \in N} w_{ij}$$

11

where w_{ij} is the normalized connection weights that $0 \leq w_{ij} \leq 1$.

Thus, each subject has four graphs in four EEG frequency bands, and each graph has extracted three graph theory measures to detect the ADHD.

3 Results

3.1 Statistical analysis

All data were presented as mean (\pm SEM) by the SEM algorithm. SEM represents the relative error between the sample mean and the overall mean [32]. The smaller the SEM value, the smaller the sampling error. The SEM algorithm is shown as follow:

$$\mu_x = \frac{\sum_{i=1}^n X_i}{n}$$

12

$$s = \sqrt{\frac{\sum_{i=1}^n (X_i - \mu_x)^2}{n - 1}}$$

13

$$SE_{\mu_x} = \frac{s}{\sqrt{n}}$$

14

where x is the sample, n is the number of the sample, μ_x is the sample mean, s is the sample standard deviation and the SE_{μ_x} is the SEM result. Comparing the statistical analysis result to find the most obviously difference in three graph theoretical measures of four EEG frequency bands.

3.2 Clustering Coefficient

Using the SEM algorithm to do the statistical analysis for the average clustering coefficient, the result Table 1. Here we found the HC groups is greater than the ADHD groups obviously in each frequency band.

Table 1
The Statistical results of average clustering coefficient between ADHD and HC

	Delta band	Theta band	Alpha band	Beta band
ADHD	0.058 ± 0.003	0.056 ± 0.003	0.054 ± 0.003	0.060 ± 0.003
HC	0.077 ± 0.005	0.074 ± 0.005	0.075 ± 0.005	0.088 ± 0.004

3.3 Nodal Efficiency

Here, we found in delta band the nodal efficiency provided the most different features and the least error because the mean value between the ADHD and HC, and the smallest value of the SEM. Focus on this frequency band, the F3 and Fz points which represent the left forehead and the forehead midline point have significant differences. Comparing the healthy children, the ADHD children has very high ability of exchange information in left forehead but poor at the forehead middle part.

Table 2
The Statistical results of nodal efficiency between ADHD and HC

	Delta band	Theta band	Alpha band	Beta band
F3 - ADHD	0.079 ± 0.008	0.086 ± 0.009	0.089 ± 0.008	0.103 ± 0.008
F3 - HC	0.063 ± 0.008	0.066 ± 0.008	0.071 ± 0.008	0.094 ± 0.011
P3 - ADHD	0.072 ± 0.006	0.087 ± 0.008	0.095 ± 0.010	0.120 ± 0.013
P3 - HC	0.062 ± 0.009	0.068 ± 0.009	0.071 ± 0.009	0.108 ± 0.015
Fz - ADHD	0.014 ± 0.004	0.015 ± 0.005	0.014 ± 0.004	0.026 ± 0.006
Fz - HC	0.031 ± 0.009	0.031 ± 0.009	0.034 ± 0.009	0.057 ± 0.011
Cz -ADHD	0.018 ± 0.003	0.016 ± 0.003	0.020 ± 0.003	0.029 ± 0.006
Cz - HC	0.029 ± 0.005	0.029 ± 0.005	0.030 ± 0.005	0.048 ± 0.012
Pz - ADHD	0.014 ± 0.003	0.012 ± 0.002	0.014 ± 0.003	0.029 ± 0.007
Pz - HC	0.026 ± 0.006	0.026 ± 0.006	0.025 ± 0.006	0.039 ± 0.009

3.4 Degree Centrality

In Table 3, Delta band also proposed a least error. Comparing the HC groups, we found that ADHD groups has most difference in F3 and Fz in measure of degree centrality. That means the left forehead of ADHD children has more correlation with other brain regions, but this ability is poor in the forehead middle part.

Table 3
The Statistical results of degree centrality between ADHD and HC.

	Delta band	Theta band	Alpha band	Beta band
F3 - ADHD	1.238 ± 0.153	1.341 ± 0.172	1.359 ± 0.158	1.475 ± 0.145
F3 - HC	0.896 ± 0.129	0.939 ± 0.129	0.997 ± 0.133	1.306 ± 0.198
P3 - ADHD	1.056 ± 0.115	1.300 ± 0.152	1.434 ± 0.170	1.781 ± 0.240
P3 - HC	0.855 ± 0.151	0.955 ± 0.163	0.994 ± 0.165	1.539 ± 0.253
Fz - ADHD	0.134 ± 0.056	0.143 ± 0.065	0.135 ± 0.056	0.263 ± 0.065
Fz - HC	0.378 ± 0.145	0.378 ± 0.144	0.398 ± 0.142	0.764 ± 0.191
Cz - ADHD	0.210 ± 0.049	0.193 ± 0.047	0.205 ± 0.046	0.335 ± 0.072
Cz - HC	0.310 ± 0.068	0.299 ± 0.067	0.295 ± 0.067	0.618 ± 0.200
Pz - ADHD	0.115 ± 0.024	0.117 ± 0.023	0.121 ± 0.022	0.319 ± 0.091
Pz - HC	0.267 ± 0.086	0.264 ± 0.088	0.252 ± 0.087	0.455 ± 0.132

4 Discussion

In EEG signal analysis, multi-channel analysis can provide the structure function relationships between different areas of the brain which single channel approaches ignore [33]. Here, we construct the brain network using effective connectivity technique to describe the brain activity in whole brain network. It can be notice from Fig. 3, PSI algorithm support casual information in connectivity analysis. In previous study, functional connectivity revealed that the ADHD patient exist the difference in forehead part comparing with the HC. Here, we use the PSI provide more evidence of the ADHD in causal relationship of each region of interest in the whole brain.

The nature of EEG signal is dynamic, and it provides a high resolution in times series. The PSI method (Figs. 2 and 3) is used to combine information about different frequencies. The classic PSI measure are based on the power spectrum in frequency domain, here we used MVAR model to represent the power

spectrum analysis. The MVAR model overcome the limitation of the classic PSI method that the poor resolution in frequency domain for short time dataset. The MVAR-PSI method propose in our study is more helpful in dynamic analysis of brain activity. We used the MVAR-PSI method construct the effective connectivity in each frequency band.

Graph theoretical analysis as the most popular mathematic tools of brain network analysis is used in this study. Though the graph theory analysis, the features of ADHD is described clustering coefficient, nodal efficiency and degree centrality of specific brain regions in Tables 1, 2 and 3. Due to MVAR-PSI method provided the more information in the graphs such as the casual information and dynamic features, so we got more findings and understanding of ADHD in our research.

5 Conclusions And Future Work

This research proposed a new method to identify the ADHD children using EEG signals and effective connectivity techniques. The original EEG data is pre-filtered and divided into Delta, Theta, Alpha and Beta bands. And then, the effective connectivity graphs are constructed by applying ICA, MVAR model and PSI. The measures of clustering coefficient, nodal efficiency and degree centrality in graph theory are used to extract features from these graphs. Statistical analysis based on the SEM are employed to evaluate the graph theory measures in each frequency band. The results show a decreased average clustering coefficient in whole frequency bands for ADHD subjects. Also, in delta band, ADHD children has very high ability of exchange information in left forehead but poor at the forehead middle part. Moreover, left forehead of ADHD children has more correlation with other brain region, but this ability is poor in the forehead middle part.

In this research, just 19 channels EEG data were used which could not include more details in brain regions. In addition, the visual attention task of EEG collection is simple, a more complex task might find more different features between ADHD subjects and HC subjects. Furthermore, the activity-dependent fluctuations in connectivity is not consider in this study, we will add a dynamic model in connectivity analysis in the future.

6. Declarations

Acknowledgments

We acknowledge the material support by Ali Motie Nasrabadi, Armin Allahverdy, Mehdi Samavati, Mohammad Reza Mohammadi shared on the IEEE Data port (DOI: 10.21227/rzfh-zn36).

Availability of data and materials

The material of EEG ADHD data and HC data files are accessible download from IEEE DataPort (DOI: 10.21227/rzfh-zn36).

Funding

This research has no funding.

Authors' contributions

MKS designs the experiment and write this paper. PW, YL and BS helps to check the paper and improve some details of the experiment.

Competing interests

The authors declare that the research was conducted in the absence of any commercial or financial relationships.

References

1. Chen H, Song Y, Li X (2019) A deep learning framework for identifying children with ADHD using an EEG-based brain network. *Neurocomputing (Amsterdam)* 356:83–96
2. Furlong S et al., *Resting-state EEG Connectivity in Young Children with ADHD*. *Journal of clinical child and adolescent psychology*, 2020: p. 1–17
3. Fair DA et al (2012) Distinct neural signatures detected for ADHD subtypes after controlling for micro-movements in resting state functional connectivity MRI data. *Front Syst Neurosci* 6:80
4. Sato JR et al (2012) Abnormal brain connectivity patterns in adults with ADHD: a coherence study. *PloS one* 7(9):e45671
5. Heinrichs-Graham E et al (2014) Pharmacological MEG evidence for attention related hyper-connectivity between auditory and prefrontal cortices in ADHD. *Psychiatry Research: Neuroimaging* 221(3):240–245
6. Pereda E et al (2018) The blessing of Dimensionality: Feature Selection outperforms functional connectivity-based feature transformation to classify ADHD subjects from EEG patterns of phase synchronisation. *PloS one* 13(8):e0201660
7. Kyeong S et al (2015) A New Approach to Investigate the Association between Brain Functional Connectivity and Disease Characteristics of Attention-Deficit/Hyperactivity Disorder: Topological Neuroimaging Data Analysis. *PloS one* 10(9):e0137296
8. Ishii R, Naito Y (2020) EEG connectivity as the possible endophenotype in adult ADHD. *Clinical neurophysiology* 131(3):750–751
9. Li Y et al (2016) High-resolution time-frequency analysis of EEG signals using multiscale radial basis functions. *Neurocomputing (Amsterdam)* 195:96–103
10. Allahverdy A, Nasrabadi AM, Mohammadi MR, *Detecting ADHD children using symbolic dynamic of nonlinear features of EEG*. 2011, IEEE. p. 1–1

11. Samavati M, Nasrabadi AM, Mohammadi MR, *Automatic minimization of eye blink artifacts using fractal dimension of independent components of multichannel EEG*. 2012, IEEE. p. 1576–1578
12. Mohammadi MR et al (2016) EEG classification of ADHD and normal children using non-linear features and neural network. *Biomedical Engineering Letters* 6(2):66–73
13. Smit DJA et al (2008) Heritability of “small-world” networks in the brain: A graph theoretical analysis of resting-state EEG functional connectivity. *Hum Brain Mapp* 29(12):1368–1378
14. Adebimpe AA et al (2015) ID 234 – Brain network analysis of EEG functional connectivity in patients with benign childhood epilepsy with centro-temporal spikes. *Clin Neurophysiol* 127(3):e60–e60
15. Lee D et al (2018) Effects of an Online Mind-Body Training Program on the Default Mode Network: An EEG Functional Connectivity Study. *Scientific reports* 8(1):16935–16938
16. Rotondi F et al (2015) Altered EEG resting-state effective connectivity in drug-naïve childhood absence epilepsy. *Clin Neurophysiol* 127(2):1130–1137
17. Wang C et al (2015) Graph theoretical analysis of EEG effective connectivity in vascular dementia patients during a visual oddball task. *Clin Neurophysiol* 127(1):324–334
18. Adamczyk P, Wyczesany M, Daren A (2019) Dynamics of impaired humour processing in schizophrenia – An EEG effective connectivity study. *Schizophr Res* 209:113–128
19. Marinazzo D et al., *Nonlinear connectivity by Granger causality*. *NeuroImage (Orlando, Fla.)*, 2011. **58**(2): p. 330–338
20. Zheng L et al (2017) Altered effective brain connectivity at early response of antipsychotics in first-episode schizophrenia with auditory hallucinations. *Clinical neurophysiology* 128(6):867–874
21. Pagnotta MF, Plomp G (2018) Time-varying MVAR algorithms for directed connectivity analysis: Critical comparison in simulations and benchmark EEG data. *PloS one* 13(6):e0198846
22. Liu J et al., *Complex Brain Network Analysis and Its Applications to Brain Disorders: A Survey*. Complexity (New York, N.Y.), 2017. **2017**: p. 1–27
23. Cao J et al (2018) Investigation of brain networks in children with attention deficit/hyperactivity disorder using a graph theoretical approach. *Biomed Signal Process Control* 40:351–358
24. Evangelos A, Constantinos S (2020) Construction of functional brain connectivity networks from fMRI data with driving and modulatory inputs: an extended conditional Granger causality approach. *AIMS neuroscience* 7(2):66–88
25. Haufe S et al., *A critical assessment of connectivity measures for EEG data: A simulation study*. *NeuroImage (Orlando, Fla.)*, 2013. **64**: p. 120–133
26. Chai MT et al., *Exploring EEG Effective Connectivity Network in Estimating Influence of Color on Emotion and Memory*. *Frontiers in neuroinformatics*, 2019. **13**
27. Seppanen JM et al., *Analysis of electromechanical modes using multichannel Yule-Walker estimation of a multivariate autoregressive model*. 2013, IEEE. p. 1–5
28. Lei CL et al., *Thermal Error Robust Modeling for High-Speed Motorized Spindle*. 2012. p. 961–965

29. Gomez C et al., *Assessment of EEG Connectivity Patterns in Mild Cognitive Impairment Using Phase Slope Index*. 2018 40th Annual International Conference of the IEEE Engineering in Medicine and Biology Society (EMBC), 2018. **2018**: p. 263–266
30. Akbarian B, Erfanian A (2020) A framework for seizure detection using effective connectivity, graph theory, and multi-level modular network. *Biomed Signal Process Control* 59:101878
31. Rubinson M et al (2019) Electroencephalography Functional Networks Reveal Global Effects of Methylphenidate in Youth with Attention Deficit/Hyperactivity Disorder. *Brain connectivity* 9(5):437–450
32. Lee DK, In J, Lee S (2015) Standard deviation and standard error of the mean. *Korean journal of anesthesiology* 68(3):220–223
33. Shen C-P et al (2013) A physiology-based seizure detection system for multichannel EEG. *PloS one* 8(6):e65862

Figures

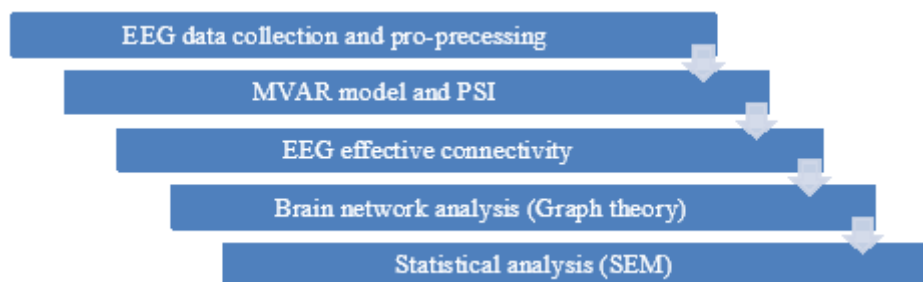


Figure 1

A framework of an effective connectivity analysis in ADHD and HC

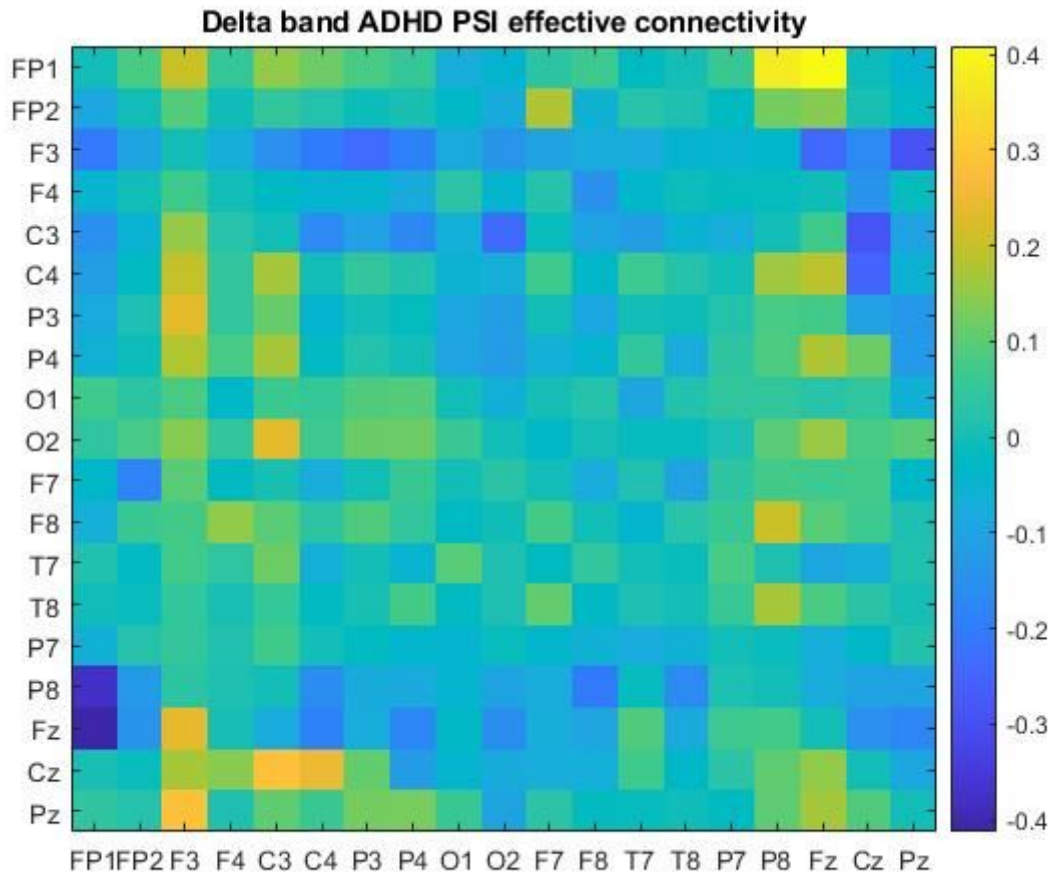


Figure 2

PSI effective connectivity matrix in delta band (0.5 – 4Hz) for ADHD subject

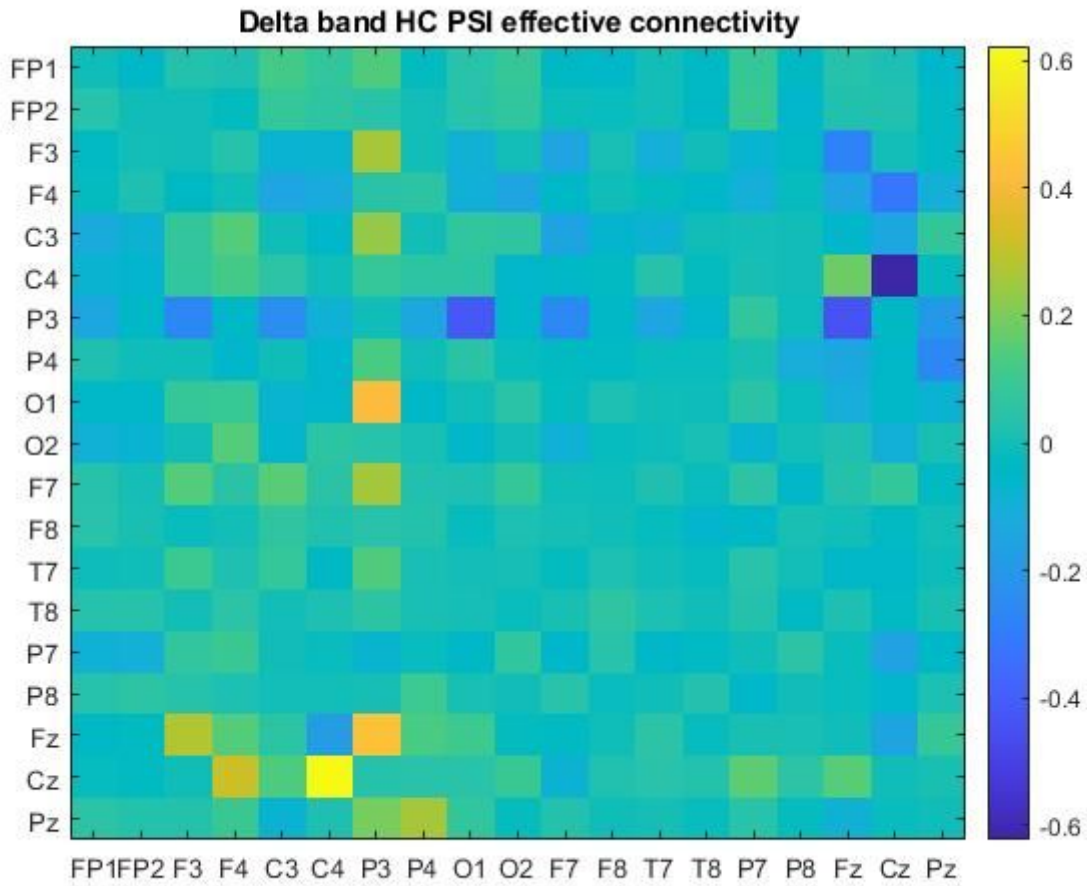


Figure 3

PSI effective connectivity matrix in delta band (0.5 – 4Hz) for HC subject